Genetics

Apolipoprotein E particle size is increased in Alzheimer's disease

Thomas J. Nelson[a,*], Abhik Sen[b]

[a]*Center for Neurodegenerative Diseases, Rockefeller Neuroscience Institute, West Virginia University, Morgantown, WV, USA*
[b]*George & Anne Ryan Institute For Neuroscience, University of Rhode Island, Kingston, RI, USA*

Abstract

Introduction: Apolipoprotein E4 (apoE4) is the predominant risk factor for late-onset Alzheimer's disease (AD), but the question of which structural differences might explain its effect remains unclear.

Methods: We compared high-density lipoprotein–like apoE particles from 12 AD and 10 control patients using size-exclusion chromatography.

Results: ApoE particles from patients genotyped as ε4/ε4 were 2.2 ± 0.3 times as massive as particles from ε3/ε3 control subjects and 1.4 ± 0.1 times as massive as particles from ε3/ε3 AD patients. The increased particle size was not because of incorporation of amyloid β or apoE proteolysis products. Particles from AD patients genotyped as ε3/ε3 were 1.59 ± 0.27 times as massive as ε3/ε3 control subjects.

Discussion: Increased particle size in AD is affected by *APOE* genotype and by disease-related differences in assembly or stability. These differences suggest that lipoprotein assembly or stability in AD brain plays an important role in determining apoE4 pathogenicity.

© 2018 The Authors. Published by Elsevier Inc. on behalf of the Alzheimer's Association. This is an open access article under the CC BY-NC-ND license (http://creativecommons.org/licenses/by-nc-nd/4.0/).

Keywords: ApoE; apolipoprotein E; HDL; Alzheimer's disease; Size-exclusion HPLC

1. Introduction

In the human population, apolipoprotein E (apoE) is found in three major isoforms, which differ at two amino acid positions. The *APOE* ε4 allele, found in 13% of the general population, is the predominant risk factor for late-onset Alzheimer's disease (AD), whereas *APOE* ε2, found in approximately 10% of the population, confers protection, and *APOE* ε3, present in most patients, provides an intermediate level of risk [1]. One ε4 allele increases the risk over ε3 by 3.7-fold; two ε4 alleles increase the risk by 12-fold [2]. In patients with ε4/ε4, 91% eventually suffer from AD, whereas little AD is seen in ε2/ε2 subjects. ApoE2 is also associated with less cognitive decline during aging [3]. In addition, two ε4 alleles reduce the age of disease onset by 15 years. The question of how apoE4 contributes to AD is therefore of major public health significance.

Astrocytes, the principal exporters of apoE in the brain, undergo complex changes early in the course of AD [4]; however, neurons and microglia also produce significant amounts of apoE. ApoE expression is greatly increased after traumatic brain injury, and apoE strongly promotes synaptogenesis [5]. *APOE* ε4 transgenic mice develop more brain atrophy and neurodegeneration and exhibit astrocytic activation and tumor necrosis factor α (TNF-α) release, suggesting a toxic gain of function [6]. These results suggest that apoE is intimately involved in neuronal maintenance, growth, and repair. However, no explanation has yet emerged that could explain the protective effects of apoE2 or the high prevalence of late-onset AD in *APOE* ε4/ε4 patients.

The strong risk effect of apoE4 is reflected in the fact that the three-dimensional structure of apoE differs greatly among the three major isoforms. Nuclear magnetic resonance and X-ray crystallographic studies of the receptor-binding NH_2 domain of apoE3 (residues 1–191) showed that apoE exists as a four-helix bundle, with basic amino acids clustered onto a surface patch (residues 136–150) of one helix [7,8]. The linker between the NH_2 and CO_2H-terminal domains becomes less protease-sensitive on lipid binding. Molecular modeling studies have shown [9] that apoE4 is topologically less rigid than apoE3 and can exist in a "molten globule" state.

Nuclear magnetic resonance [7] and hydrogen-deuterium exchange mass spectrometry studies [10–12] also showed that Arg112 interacts with Lys95, leading to a marked change in protein folding. On the basis of these and other structural studies, phthalazinone derivatives known as "correctors" were designed in an attempt to inhibit this interaction and convert apoE4 to an E3-like configuration [13]. However, apoE is not usually found free in solution, but is lipidated and assembled in large, stable high-density lipoprotein–like particles. Lipidation has a major contribution to apoE configuration; for example, it enables apoE4 to adopt a closed conformation [14], which somewhat mimics the effect of the phthalazinones. ApoE4 is less lipidated in cerebrospinal fluid [15], but is the most lipidated form in astrocytes [14]. Thus, modifying the lipidation state of apoE4 particles may be an alternative means of mitigating AD pathology.

Before proceeding further, however, it is necessary to understand how lipidation and particle composition are affected in AD, and how particle structure and composition affect apoE4 pathogenicity. Most previous studies have examined apoE using native gel electrophoresis or KBr gradient ultracentrifugation. These studies showed that in cerebrospinal fluid, *APOE* ε2/ε3 subjects had larger high-density lipoprotein–like complexes than *APOE* ε4/ε4 subjects, suggesting possible differences in transport or clearance as well as abundance. In this study, we used size-exclusion high-pressure liquid chromatography (HPLC) to characterize the particle size profile in AD brain and human APOE–targeted replacement mice. We found that apoE4 particles exhibit significant size differences that depend not only on *APOE* genotype, but on disease state in patients with identical genotype as well.

2. Methods

2.1. Cell culture and astrocyte-conditioned medium

Human-derived SH-SY5Y cells were cultured in Dulbecco's Modified Eagle Medium/ Ham's Nutrient Mixture F-12 (DMEM/F12K) + 10% FCS and differentiated to a neuronal phenotype by incubation in neuronal medium (ScienCell 1521) for 1 week. This medium contains Neuronal Growth Supplement (ScienCell 1562), which provides retinyl acetate (final concentration = 0.01 μg/mL) and growth factors, hormones, and antioxidants necessary for neuronal cell culture. This treatment produced cells comparable to other retinoic acid differentiation protocols such as that described by Encinas et al. [16]. Differentiated cells were used within 3 days. Medium could be replaced with phosphate-buffered saline (PBS) for up to 1 hour. For longer-term experiments, the continued presence of medium was necessary for cell survival. Human astrocytes (ScienCell) were cultured in Astrocyte Medium containing 2% fetal bovine serum, astrocyte growth supplement (ScienCell 1852), and penicillin/streptomycin. After expansion, astrocytes were replated in serum-free medium (DMEM/F12, 1:1) and serum-free astrocyte-conditioned medium was collected after 48 hours and stored at −20°C.

2.2. Size-exclusion HPLC

To measure apoE particle size, autopsy samples from AD temporal lobe were homogenized by sonication in 9 vol of $1\times$ PBS containing protease inhibitor cocktail (Roche) and centrifuged at $100,000g$ for 20 minutes at 4°C. The supernatant was injected (5–25 μL) onto a 4×300 mm MabPac size-exclusion chromatography HPLC column (Thermo) eluted with 0.1 M sodium phosphate + 0.1 M sodium sulfate, pH 6.65, at a flow rate of 0.2 mL/min, and 0.2-minute fractions were collected. The fractions were blotted onto a nitrocellulose membrane, stained with anti-apoE antibody and alkaline-phosphatase–linked secondary antibody, and developed with 5-bromo-4-chloro-3-indolyl phosphate (BCIP)/nitro blue tetrazolium (NBT). The blots were imaged while still wet and spot densities were measured using the fixed-diameter circle densitometry algorithm in Imal, which uses fuzzy k-means clustering to calculate the background value from the surrounding area for each measurement. Retention time was calculated by smoothing the chromatograms with a 21-point Gaussian convolution filter, then numerically differentiating the curve and determining the *x*-axis coordinate of the zero intercept. Molecular weight was estimated from an exponential curve fitted to the data points obtained from protein standards. Particle size was estimated using protein molecular weight (MW) standards and converted to volume using a lipoprotein density of 1.23 [17] using an established formula [18].

2.3. Genotyping

Genomic DNA was isolated from cultured cells or autopsy samples using DNAzol or a Qiagen QIAmp extraction kit. Cells were washed with PBS and lysed

in DNAzol added at 0.1 mL/cm^2 culture plate area. Tissue was lysed with 1 mL DNAzol per 25 mg tissue. Genomic DNA was ethanol-precipitated and *APOE* genotype was determined using TaqMan end point single-nucleotide polymorphism (SNP) genotyping in a Roche LightCycler 480 using VIC/FAM-labeled probes rs429358 and rs7412.

2.4. Gas chromatography

Combined samples (0.2 mL) from multiple injections of human high-speed temporal lobe extract on size-exclusion HPLC were extracted with 0.2 mL hexane and evaporated to dryness. Hexane (0.1 mL) and N, O-bis(trimethylsilyl) trifluoroacetamide (BSTFA) (0.1 mL) were added. The samples were incubated in a sealed vial with Teflon cap at 70°C for 20 minutes and 1–5 μL were injected into a 30 m Restek Rxi-Sil MS column in a Shimadzu GC-2014 gas chromatograph equipped with a flame ionization detector and eluted with a temperature gradient from 220°C to 300°C. Cholesterol eluted at 18.30 minutes and peak areas were quantitated using custom data analysis software (Xdata).

2.5. Statistical analysis

Experiments in which two or more factors are measured were analyzed by one-way analysis of variance (ANOVA), followed by Tukey Honest Significant Difference multiple comparisons of means (95% familywise confidence level) using R. Kinetic parameters (Kd) and inhibition constants were calculated by nonlinear least-squares analysis using custom software (Xdata). Other statistics were calculated in R using the two-tailed Welch two-sample *t* test. One-way robust repeated measures ANOVAs were calculated in R by the method of Wilcox [19].

2.6. Amyloid β oligomers

Synthetic (amyloid β 1–42) Aβ$_{1-42}$ was converted to monomers by incubating for 18 hours at 4°C with 1,1,1,3,3,3-hexafluoropropanol followed by 3 hours of incubation at 37°C. The solvent was then removed by lyophilization. The monomers were dissolved in PBS at 1 μM, transferred to a 1.5 mL polypropylene centrifuge tube, and oligomerized into amylospheroidal oligomers by rotating at 1 rpm at 4°C for 14 hours to produce highly toxic oligomers [20,21].

2.7. Oxidized lipids

Peroxidized egg yolk phosphatidyl choline was prepared by the method of Bielicki et al. [22]. Egg yolk phosphatidyl choline (10 mg) was incubated with 200 nmol CuCl$_2$ in 200 μL ethanol for 1 h at 37°C, then extracted with ethyl acetate/hexane (1:1), washed with 20 mM EDTA in 0.5 mL Tris-HCl pH 8.0 to remove any remaining Cu^{2+}, evaporated, and dissolved in 50 μL ethanol. The peroxidized lipid solution was added at a final concentration of 18 μg/mL to astrocytes in six-well plates containing 2 mL of Astrocyte Medium.

2.8. Animals

Human *APOE*3 and *APOE*4–targeted replacement mice (male, 1548-M and 1549-M, B6.129P2-Apoe$^{tm3(APOE*3)Mae}$ N8 or B6.129P2-Apoe$^{tm3(APOE*4)Mae}$ N8) were purchased from Taconic. Animals were euthanized in a flow-controlled CO$_2$ inhalation chamber in accordance with American Veterinary Medical Association guidelines and brain tissue was homogenized under the same conditions as human autopsy samples. All animal experiments were carried out in accordance with the National Institutes of Health guide for the care and use of Laboratory animals (NIH Publications No. 8023, revised 1978).

3. Results

3.1. ApoE-containing particles are larger in patients with AD

Size exclusion HPLC of temporal lobe proteins from 12 AD and 10 age-matched control subjects obtained at autopsy revealed that apoE-containing lipoprotein particles extracted from AD brain were significantly larger than particles from control subjects (ANOVA *F* (4,15) = 0.0091; Fig. 1A). This is equivalent to a 1.82 ± 0.26–fold higher MW (*P* < .001, Table 1.) ApoE3 in unaffected (control) patients showed the greatest abundance of 13.0 nm diameter particles, corresponding to an MW of 790 ± 110 kDa. ApoE particles in patients with AD genotyped as ε3/ε3 and ε3/ε4 were larger, with modal values of approximately 14.8 ± 0.4 and 15.3 ± 0.7 nm, whereas apoE particles from patients genotyped as ε4/ε4 were even larger, with a modal value at 16.5 ± 0.3 nm, corresponding to an MW of 1750 ± 100 kDa [18] (*P* < .001, Table 1). Thus, particles in ε4/ε4 AD patients were 2.2 ± 0.3 times as massive as particles in ε3/ε3 control subjects. Significant amounts of apoE monomers were also present in all samples, whereas little signal was detected in low-MW regions corresponding to fragmented apoE.

3.2. Increased particle size is not due to apoE isoform alone

Particles from patients with AD genotyped as *APOE* ε3/ε3 were 1.59 ± 0.27 times as massive as particles from *APOE* ε3/-ε3 control subjects (n = 4 AD, n = 8 control, *P* = .026). This indicates that increased particle size is not only due to apoE isoform alone, but also shows that disease-related differences in the structure or composition of apoE high-density lipoprotein–like particles leading to increased particle size may play a significant role in determining AD pathogenicity.
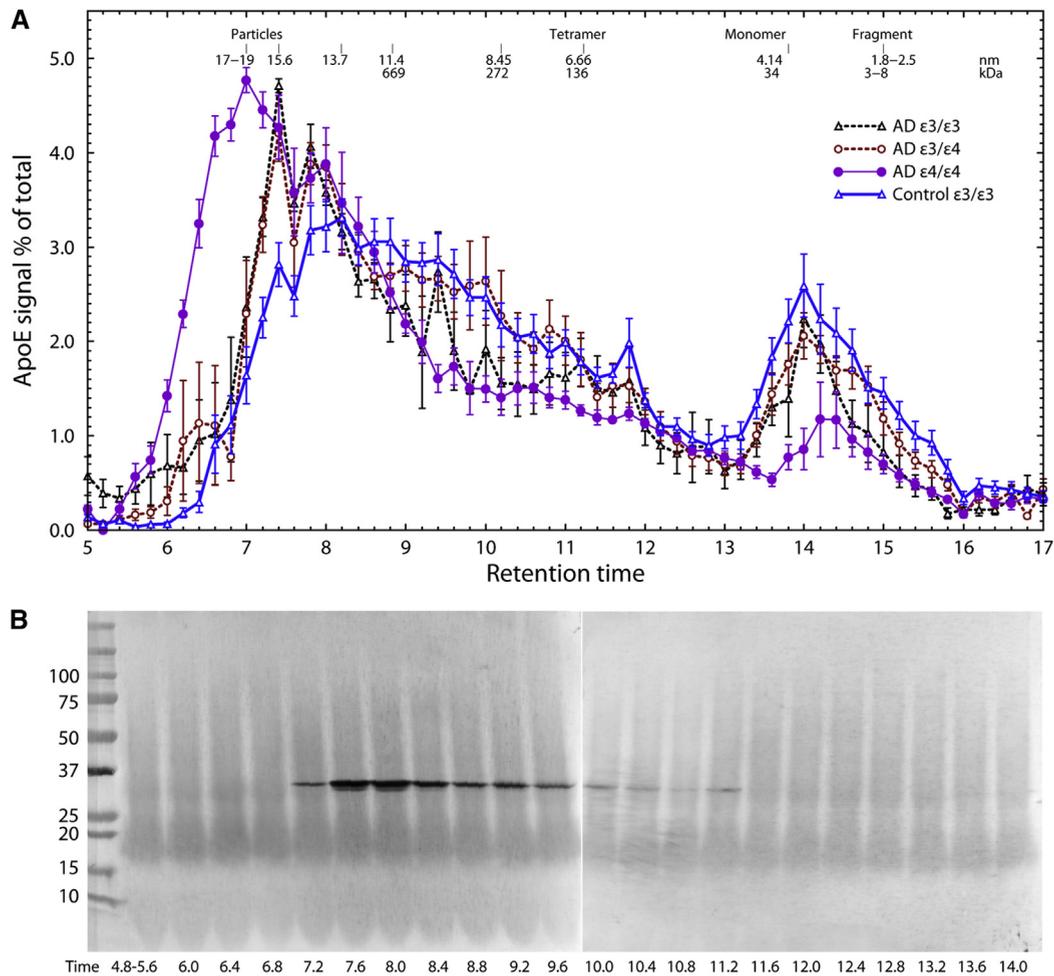
Fig. 1. (A) Size-exclusion chromatography of apoE particles in control and AD temporal lobe segregated by genotype. HPLC fractions were stained with anti-apoE monoclonal antibody (sc-13521) and analyzed densitometrically. Chromatograms are normalized to constant area. Values are mean $\pm$ SEM (N = 8 control ε3/ε3, 4 AD ε3/ε3, 5 AD ε3/ε4, 3 AD ε4/ε4). Robust repeated measures ANOVA F (4, 15) = 5.3, P = .0091. One way ANOVA F (4, 15) = 5.01, P = .0091. (B) Western blot of apoE HPLC fractions (autopsy sample, aged control). Abbreviations: AD, Alzheimer's disease; ANOVA, analysis of variance; apoE, apolipoprotein E; SEM, standard error of the mean.

Some researchers have suggested that apoE4 is more susceptible than apoE3 to proteolysis, and that proteolytic fragments from apoE4 may produce toxic effects [23–25]. Fig. 1B confirms that the apoE in our samples was largely undegraded, indicating that the different sizes are not because of the presence of degraded apoE. This was additionally confirmed by Western blots of crude homogenates (not shown). In all patients, approximately 50% to 75% of the apoE was at the MW corresponding to sialylated apoE (apparent MW 35.3 kDa) and 25% to 50% unsialylated (33.6 kDa). The particles contained cholesterol; the distribution of

Table 1
Subject description and effect of AD and genotype on apoE particle size

Group	n	Age	Braak stage	t_R (min)	Diameter (nm)	MW (kDa)	MW ratio	P value
All control	10	83.0 ± 2.2	0.0	8.31 ± 0.17	13.0 ± 0.5	850 ± 90	1.00 ± 0.15	—
All AD	12	80.5 ± 2.1	5.2 ± 0.2	7.41 ± 0.17	15.8 ± 0.5	1530 ± 16	1.82 ± 0.26	<.001
Con ε3/ε3	8	82.5 ± 2.7	0.0	8.42 ± 0.20	12.7 ± 0.6	790 ± 110	1.00 ± 0.21	—
AD ε3/ε3	4	79.2 ± 4.2	5.0 ± 0.4	7.73 ± 0.14	14.8 ± 0.4	1250 ± 110	1.59 ± 0.27	.026
AD ε3/ε4	5	85.4 ± 1.7	5.4 ± 0.2	7.56 ± 0.27	15.3 ± 0.7	1380 ± 210	1.75 ± 0.37	.019
AD ε4/ε4	3	74.0 ± 3.6	5.1 ± 0.2	7.21 ± 0.09	16.5 ± 0.3	1750 ± 100	2.22 ± 0.35	<.001

Abbreviations: AD, Alzheimer's disease; apoE, apolipoprotein E; MW, molecular weight; SE, standard error.
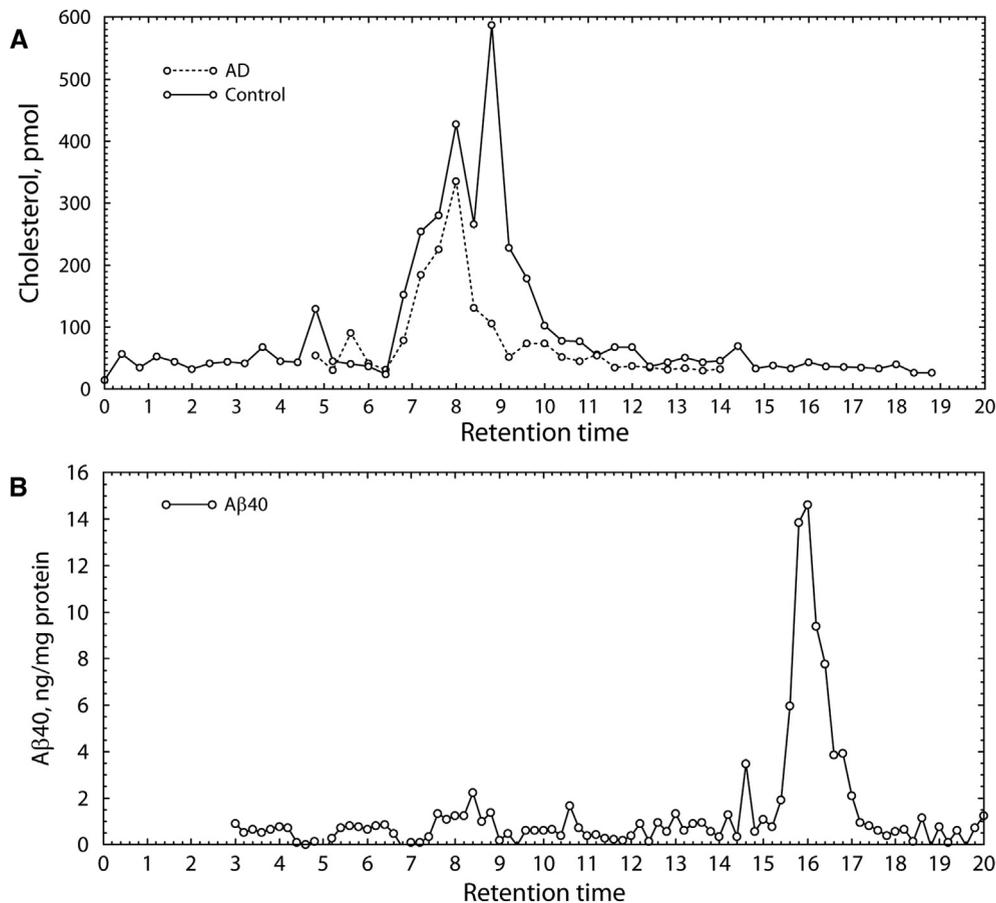NOTE. All values are the mean $\pm$ SE. t_R = retention time. P values (two-tailed) are calculated from MW.

Fig. 2. (A) Cholesterol and Aβ content of apoE particles from patient with AD and aged control patient. ApoE was fractionated by size-exclusion HPLC and cholesterol content in each fraction was measured by gas chromatography. (B) Aβ$_{40}$ in size exclusion HPLC fractions of extract from human patient with AD. Aβ$_{40}$ was measured by fluorescent enzyme-linked immunosorbent assay. Aβ$_{40}$ was found only in the low-MW region (16 minutes, $\approx$ 5–10 kDa), whereas apoE particles ($t_R \approx$ 8–10 minutes) contained no detectable Aβ$_{40}$ (<1 pg/mL). Abbreviations: Aβ, amyloid β; AD, Alzheimer's disease; apoE, apolipoprotein E; MW, molecular weight.

cholesterol paralleled the size distribution of apoE (Fig. 2A). Little or no cholesterol was associated with monomeric apoE.

Some evidence suggests that apoE may participate in clearance of Aβ. Thus, the possibility was considered that the higher MW in ε4/ε4 patients was because of the presence of Aβ. However, we did not detect any Aβ associated with authentic apoE particles in patients with AD (Fig. 2B), indicating that the larger particle size is not because of incorporation of Aβ.

3.3. ApoE3 more readily dissociates from aggregates

Fig. 1A also shows that a smaller proportion of apoE from patients genotyped as ε4/ε4 is found in monomeric form compared with control ε3/ε3, AD ε3/ε3, and AD ε3/ε4. Previous structural studies on recombinant apoE in solution have suggested that differences in dissociation of apoE aggregates reflect properties that may determine in vivo function. For example, Garai et al. [26] found that dissociation of apoE to monomers is essential for membrane binding, suggesting that physical properties

that underlie aggregation also play a role in particle stability. Native apoE forms predominantly tetramers that spontaneously disaggregate in solution. To determine whether differences in apoE protein structure could account for the larger particle size, recombinant apoE2, E3, or E4 was incubated at 35°C at 1.0 μg/mL (29 nM) in the presence of 1 μg/mL micellar cholesterol and protease inhibitors. Under these conditions, apoE3 consistently disaggregated into monomers, whereas apoE2 and apoE4 aggregates were stable for up to 4 hours, thereafter gradually precipitating onto the walls of the sample vial. By 48 hours, 70% of the apoE2 and 30% of the apoE4 disappeared from solution (Fig. 3).

3.4. ApoE particle size in APOE-targeted replacement mice

Targeted replacement mice (Taconic) exhibit reduced levels of brain-derived neurotrophic factor (BDNF) [27,28] and TNF-α [6,29], apoE isoform–dependent inflammation [30], and impaired spatial learning [31].
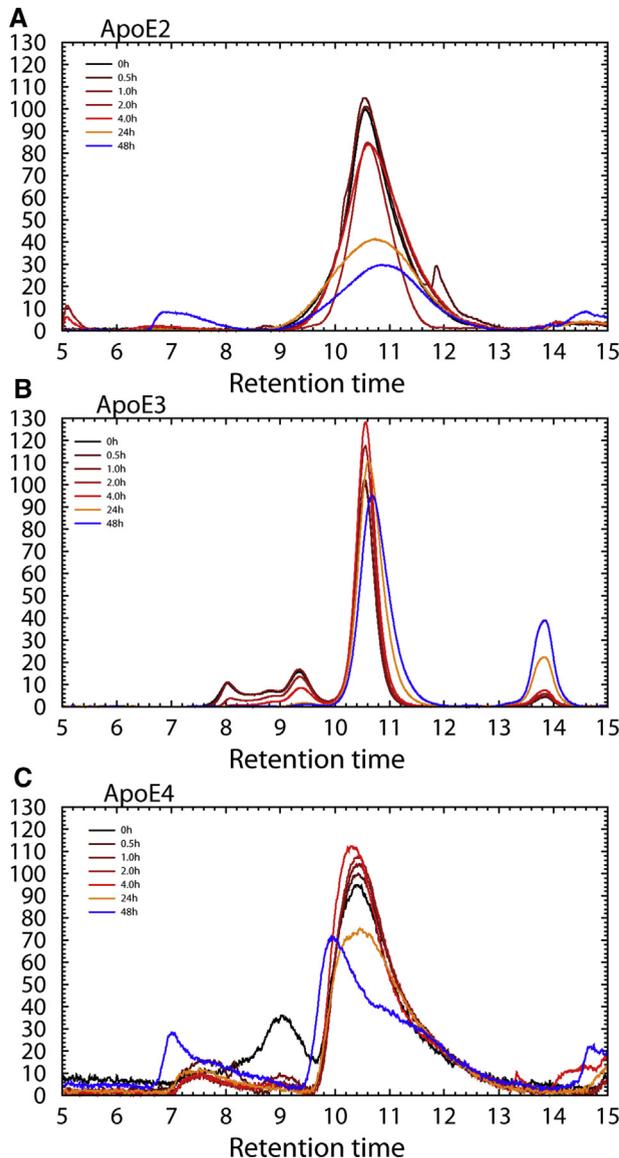
Fig. 3. Size exclusion HPLC A_{280} profiles of 29 nM recombinant (A) apoE2, (B) apoE3, and (C) apoE4 incubated at 35°C with protease inhibitors and 2.59 μM micellar cholesterol. ApoE3 tetramers slowly disaggregated to monomers, whereas apoE4 remained intact, indicating that structural differences among apoE isoforms affect its oligomerization properties. This result shows that apoE3 dissociates faster, indicating differences in binding properties. (Typical results of three to four experiments with each isoform shown.) Abbreviation: apoE, apolipoprotein E.
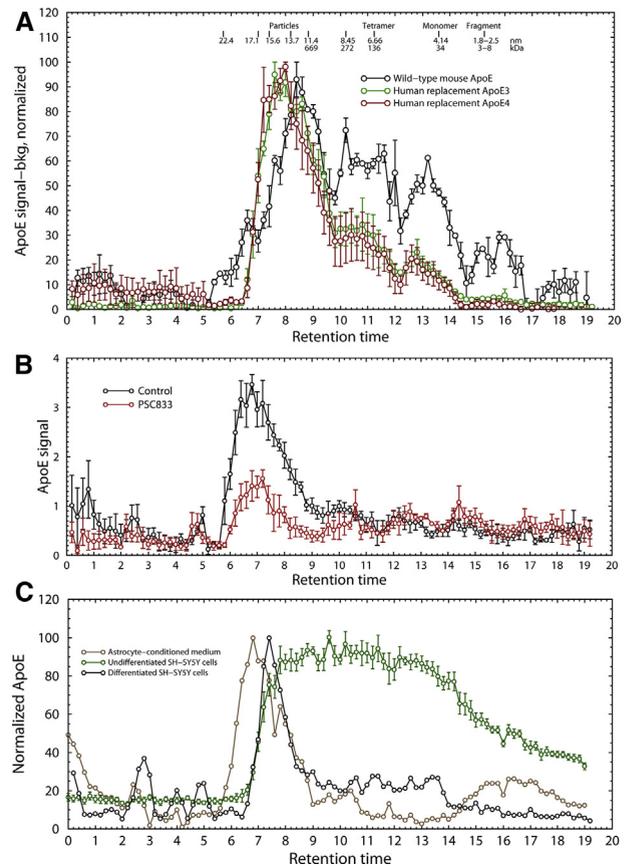

Fig. 4. (A) ApoE particle size exclusion profile in transgenic targeted replacement *APOE* mice. Black = wild-type murine apoE, green = human transgenic replacement apoE3, red = human transgenic replacement apoE4 ($n = 3$). (B) ApoE particle size profile in human astrocytes treated with PSC833, an ABCA1 inhibitor ($n = 3$). (C) Normalized size exclusion HPLC of apoE particles in undifferentiated human SH-SY5Y cells (green), differentiated SH-SY5Y cells (black and red), and human astrocyte-conditioned medium (brown). ApoE particles in astrocyte-conditioned medium are approximately 18 nm in diameter, identical in size to the apoE particles in ε4/ε4 AD temporal lobe. (Typical results of three experiments are shown.) Abbreviations: ABCA1, adenosine triphsphate-binding cassette transporter 1; AD, Alzheimer's disease; apoE, apolipoprotein E.

noic acid]cyclosporin D), an inhibitor of adenosine triphosphate-binding cassette transporter 1, which mediates the assembly of high-density lipoproteins, the quantity of apoE-containing particles produced by astrocytes was decreased but was no effect on particle size (Fig. 4B). Induction of A1 astrogliosis by cytokines (interleukin 1α, TNF-α, and C1q) [33], which produces marked changes in astrocyte morphology, also had no effect on particle size (Table 2). Incubation with oxidized phosphatidylcholine, a potent inhibitor of lecithin-cholesterol acyltransferase [22], produced a small but statistically significant increase in particle size, whereas 4-hydroxynonenal, a highly reactive marker of oxidative stress, at the maximum concentration consistent with cell survival (16 μM), had no effect.

Human apoE3 and E4 in targeted replacement mice had identical particle sizes (15 nm), comparable to apoE in patients with AD, whereas native mouse apoE, which is believed to structurally resemble apoE4, was approximately 13 nm in diameter, as observed by previous researchers [32], comparable in size to apoE3 in unaffected human patients, and was accompanied by smaller particles 5 to 8 nm in diameter (Fig. 4A). When human astrocytes were treated with PSC833 (6-[(2S,4R,6E)-4-methyl-2-(methylamino)-3-oxo-6-octe-

Table 2
Effect of cytokines and enzyme inhibitors on apoE particle size in human astrocytes and neuronal cells

Cells/treatment	Retention time (min)	Diameter (nm)	Molecular weight (kDa)	P value
Astrocytes	6.90 ± 0.09	17.7 ± 0.3	2160 ± 120	—
Neuronal cells	7.78 ± 0.02	14.6 ± 0.1	1200 ± 10	.0015
Astrocytes + PSC833	6.97 ± 0.06	17.4 ± 0.2	2050 ± 90	ns
Astrocytes + cytokines	6.10 ± 0.04	17.3 ± 0.2	2020 ± 60	ns
Astrocytes + oxidized lipids	6.56 ± 0.05	19.1 ± 0.2	2680 ± 80	.027
Astrocytes + 4-hydroxy-nonenal	7.15 ± 0.07	16.7 ± 0.3	1830 ± 90	ns

NOTE. Retention time was measured by differentiation of the smoothed chromatograms. *P* values are calculated relative to untreated astrocytes. Oxidized lipids were added at 18 μg/mL and 4-hydroxynonenal was added at 16 μM.

3.5. Correlation of apoE particle size and neuronal and astrocyte pathology

To determine whether the increased particle size in AD was caused by astrocyte pathology or neuronal pathology, we treated differentiated SH-SY5Y cells with $A\beta_{42}$ amylospheroids, a highly toxic oligomeric form of $A\beta$ [20,21] at 200 nM for 24 hours, or with low (1%) oxygen for 24 hours. Both the astrocytes and SH-SY5Y cells in this experiment were genotyped as ε3/ε3. No changes in apoE particle size were observed either in astrocytes or in differentiated neurons (not shown). Cultured astrocytes produced particles of 17.72 ± 0.33 nm, whereas apoE particles from neuronal cells were only 14.57 ± 0.05 nm. This means that lipoprotein particles from astrocytes are 1.8 ± 0.1 times as massive as neuronal cells. Particles of ∼15 nm diameter from astrocytes have been observed previously [32]. The particles from our astrocytes were nearly identical in size to particles from AD, but not control, autopsy samples. In contrast, undifferentiated SH-SY5Y cells produced apoE in a continuum of sizes from 1.0 to 8.8 nm, containing monomers and multimers in varying proportion (Fig. 4C). Thus, we conclude that the larger particle size in *APOE* ε4/ε4 patients with AD results from AD-specific processes, which may include an increased contribution of apoE particles from astrocytes instead of neurons.

4. Discussion

Our results show that apoE particles in AD brain have a significantly larger effective volume than control subjects. ApoE particles from ε4/ε4 AD patients were, on average, over twice as massive as particles from ε3/ε3 control subjects and 1.4 times as massive as particles from ε3/ε3 AD patients. This result confirms earlier reports that apoE4 particles from patients with AD elute more rapidly in gel filtration columns [34,35]. The largest particles (16–18 nm) are 3.2 times more abundant in patients with AD than in ε3/ε3 control subjects. The increased particle size was not because of incorporation of Aβ or apoE proteolysis products.

Lipoprotein particle size in blood plasma is affected by a number of factors, including inflammation [36], triglyceride levels, and oxidative stress [37,38]. In our cultured cells, particle size was not affected by inhibitors of lipoprotein assembly, but was strongly affected by cell type and apoE isoform, with astrocytes forming particles 1.82 ± 0.26 times as massive as neuronal cells. The particle size in APO ε4/ε4 patients was closer in size to particles produced by astrocytes, whereas particle size in unaffected patients was closer to neuronal apoE, suggesting that the larger particle size in AD could result in part from an increased contribution of apoE from astrocytes. However, the finding that particles from ε3/ε3 AD patients were significantly larger than ε3/ε3 control subjects indicates that increased particle size is not only due to apoE isoform alone, but also that AD pathology affects apoE particle size. One limitation of the present study is the possibility of postmortem changes in apoE. Although reconstituted lipoprotein particles are highly stable, the possibility cannot be ruled out that natural lipoproteins may exhibit additional heterogeneity. Future research with larger populations, preferably in genetically homogeneous cells or animals, will be needed to understand the relative mechanistic contributions of *APOE* genotype and AD.

In the brain, apoE is secreted primarily by astrocytes, but neurons also produce significant quantities of apoE [39]. Under conditions of physiological stress, neuronal apoE is upregulated. Traumatic brain injury also produces a large increase in apoE expression [40]. ApoE2 is a potent inducer of BDNF secretion in vitro, increasing secreted pro-BDNF levels in astrocytes by 48.7 times, whereas apoE3 increases it by 85.4 times, and apoE4 has no effect [41]. Exogenously applied apoE4 preferentially accumulates in membranes, suggesting that it is kinetically unable to dissociate from its receptor or from its lipid environment [41]. The larger particle size in ε4/ε4 patients and reduced ability of apoE4 to dissociate could inhibit binding or endocytosis of particles, thereby depriving neurons of adequate cholesterol for repair. Further experimentation is required to address this possibility.

These findings imply large structural and functional differences among apoE isoforms, which could account for

observed biochemical differences in AD, including dysregulation of BDNF maturation, changes in membrane properties, or changes in Aβ clearance. ApoE2 has long been recognized as a protective factor in AD, but the reason for its protection and for the increased risk associated with apoE4 has remained elusive. Much previous work has assumed that the differences were only because of differences in affinity for lipids or Aβ. Our finding that both apoE isoform and AD disease state determine particle size shows that structural differences also play an important role in AD pathogenicity.

Acknowledgments

RESEARCH IN CONTEXT

1. Systematic review: ApoE4 is the strongest risk factor for late-onset Alzheimer's disease (AD). Review of the research literature reveals that no clear understanding exists as to why *APOE* ε4 genotype contributes to AD.

2. Interpretation: We present strong evidence that apoE-containing lipoprotein particles in human brain are significantly larger in patients with AD than in unaffected patients. The difference was strongest in ε4/ε4 patients, but ε3/ε3 patients with AD also had larger particle sizes than ε3/ε3 control subjects. This indicates that AD pathology is associated with aberrations in lipoprotein assembly that may play a role in pathogenicity by interfering with cholesterol transport and ApoE signaling.

3. Future directions: These findings show that the physical properties of apoE-containing lipoprotein particles in the brain are altered in AD. Finding ways to manipulate lipoprotein structure could be a promising approach to treatment of late-onset AD.

References

[1] Ordovas JM, Litwack-Klein L, Wilson PW, Schaefer MM, Schaefer EJ. Apolipoprotein E isoform phenotyping methodology and population frequency with identification of apoE1 and apoE5 isoforms. J Lipid Res 1987;28:371–80.

[2] Corder EH, Saunders AM, Strittmatter WJ, Schmechel DE, Gaskell PC, Small GW, et al. Gene dose of apolipoprotein E type 4 allele and the risk of Alzheimer's disease in late onset families. Science 1993;261:921–3.

[3] Shinohara M, Kanekiyo T, Yang L, Linthicum D, Shinohara M, Fu Y, et al. APOE2 eases cognitive decline during aging: clinical and pre-clinical evaluations. Ann Neurol 2016;79:758–74.

[4] Beauquis J, Vinuesa A, Pomilio C, Pavia P, Galvan V, Saravia F. Neuronal and glial alterations, increased anxiety, and cognitive impairment before hippocampal amyloid deposition in PDAPP mice, model of Alzheimer's disease. Hippocampus 2014;24:257–69.

[5] Mauch DH, Nagler K, Schumacher S, Goritz C, Muller EC, Otto A, et al. CNS synaptogenesis promoted by glia-derived cholesterol. Science 2001;294:1354–7.

[6] Shi Y, Yamada K, Liddelow SA, Smith ST, Zhao L, Luo W, et al. ApoE4 markedly exacerbates tau-mediated neurodegeneration in a mouse model of tauopathy. Nature 2017;549:523–7.

[7] Chen J, Li Q, Wang J. Topology of human apolipoprotein E3 uniquely regulates its diverse biological functions. Proc Natl Acad Sci U S A 2011;108:14813–8.

[8] Wilson C, Wardell MR, Weisgraber KH, Mahley RW, Agard DA. Three-dimensional structure of the LDL receptor-binding domain of human apolipoprotein E. Science 1991;252:1817–22.

[9] Ray A, Ahalawat N, Mondal J. Atomistic insights into structural differences between E3 and E4 isoforms of apolipoprotein E. Biophys J 2017;113:2682–94.

[10] Gau B, Garai K, Frieden C, Gross ML. Mass spectrometry-based protein footprinting characterizes the structures of oligomeric apolipoprotein E2, E3, and E4. Biochemistry 2011;50:8117–26.

[11] Chetty PS, Mayne L, Lund-Katz S, Englander SW, Phillips MC. Helical structure, stability, and dynamics in human apolipoprotein E3 and E4 by hydrogen exchange and mass spectrometry. Proc Natl Acad Sci U S A 2017;114:968–73.

[12] Huang RY, Garai K, Frieden C, Gross ML. Hydrogen/deuterium exchange and electron-transfer dissociation mass spectrometry determine the interface and dynamics of apolipoprotein E oligomerization. Biochemistry 2011;50:9273–82.

[13] Chen HK, Liu Z, Meyer-Franke A, Brodbeck J, Miranda RD, McGuire JG, et al. Small molecule structure correctors abolish detrimental effects of apolipoprotein E4 in cultured neurons. J Biol Chem 2012;287:5253–66.

[14] Kara E, Marks JD, Fan Z, Klickstein JA, Roe AD, Krogh KA, et al. Isoform- and cell type-specific structure of apolipoprotein E lipoparticles as revealed by a novel Forster resonance energy transfer assay. J Biol Chem 2017;292:14720–9.

[15] Guyton JR, Miller SE, Martin ME, Khan WA, Roses AD, Strittmatter WJ. Novel large apolipoprotein E-containing lipoproteins of density 1.006-1.060 g/ml in human cerebrospinal fluid. J Neurochem 1998;70:1235–40.

[16] Encinas M, Iglesias M, Liu Y, Wang H, Muhaisen A, Cena V, et al. Sequential treatment of SH-SY5Y cells with retinoic acid and brain-derived neurotrophic factor gives rise to fully differentiated, neurotrophic factor-dependent, human neuron-like cells. J Neurochem 2000;75:991–1003.

[17] Scheffer PG, Bakker SJ, Heine RJ, Teerlink T. Measurement of low-density lipoprotein particle size by high-performance gel-filtration chromatography. Clin Chem 1997;43:1904–12.

[18] Fischer H, Polikarpov I, Craievich AF. Average protein density is a molecular-weight-dependent function. Protein Sci 2004;13:2825–8.

[19] Wilcox RR. Introduction to Robust Estimation and Hypothesis Testing. 2nd ed. Burlington, MA: Elsevier; 2005.

[20] Sen A, Alkon DL, Nelson TJ. Apolipoprotein E3 (ApoE3) but not apoE4 protects against synaptic loss through increased expression of protein kinase C epsilon. J Biol Chem 2012;287:15947–58.

[21] Hoshi M, Sato M, Matsumoto S, Noguchi A, Yasutake K, Yoshida N, et al. Spherical aggregates of beta-amyloid (amylospheroid) show high neurotoxicity and activate tau protein kinase I/glycogen synthase kinase-3beta. Proc Natl Acad Sci U S A 2003;100:6370–5.

[22] Bielicki JK, Forte TM, McCall MR. Minimally oxidized LDL is a potent inhibitor of lecithin:cholesterol acyltransferase activity. J Lipid Res 1996;37:1012–21.

[23] Huang Y, Liu XQ, Wyss-Coray T, Brecht WJ, Sanan DA, Mahley RW. Apolipoprotein E fragments present in Alzheimer's disease brains induce neurofibrillary tangle-like intracellular inclusions in neurons. Proc Natl Acad Sci U S A 2001;98:8838–43.

[24] Brecht WJ, Harris FM, Chang S, Tesseur I, Yu GQ, Xu Q, et al. Neuron-specific apolipoprotein e4 proteolysis is associated with increased tau phosphorylation in brains of transgenic mice. J Neurosci 2004;24:2527–34.

[25] Ljungberg MC, Dayanandan R, Asuni A, Rupniak TH, Anderton BH, Lovestone S. Truncated apoE forms tangle-like structures in a neuronal cell line. Neuroreport 2002;13:867–70.

[26] Garai K, Baban B, Frieden C. Dissociation of apolipoprotein E oligomers to monomer is required for high-affinity binding to phospholipid vesicles. Biochemistry 2011;50:2550–8.

[27] Maioli S, Puerta E, Merino-Serrais P, Fusari L, Gil-Bea F, Rimondini R, et al. Combination of apolipoprotein E4 and high carbohydrate diet reduces hippocampal BDNF and arc levels and impairs memory in young mice. J Alzheimers Dis 2012;32:341–55.

[28] Chhibber A, Zhao L. ERbeta and apoE isoforms interact to regulate BDNF-5-HT2A signaling and synaptic function in the female brain. Alzheimers Res Ther 2017;9:79.

[29] Lynch JR, Tang W, Wang H, Vitek MP, Bennett ER, Sullivan PM, et al. APOE genotype and an apoE-mimetic peptide modify the systemic and central nervous system inflammatory response. J Biol Chem 2003;278:48529–33.

[30] Levy O, Lavalette S, Hu SJ, Housset M, Raoul W, Eandi C, et al. ApoE isoforms control pathogenic subretinal inflammation in age-related macular degeneration. J Neurosci 2015;35:13568–76.

[31] Rodriguez GA, Burns MP, Weeber EJ, Rebeck GW. Young APOE4 targeted replacement mice exhibit poor spatial learning and memory, with reduced dendritic spine density in the medial entorhinal cortex. Learn Mem 2013;20:256–66.

[32] DeMattos RB, Brendza RP, Heuser JE, Kierson M, Cirrito JR, Fryer J, et al. Purification and characterization of astrocyte-secreted apolipoprotein E and J-containing lipoproteins from wild-type and human APOE transgenic mice. Neurochem Int 2001;39:415–25.

[33] Liddelow SA, Guttenplan KA, Clarke LE, Bennett FC, Bohlen CJ, Schirmer L, et al. Neurotoxic reactive astrocytes are induced by activated microglia. Nature 2017;541:481–7.

[34] LaDu MJ, Stine WB Jr, Narita M, Getz GS, Reardon CA, Bu G. Self-assembly of HEK cell-secreted apoE particles resembles apoE enrichment of lipoproteins as a ligand for the LDL receptor-related protein. Biochemistry 2006;45:381–90.

[35] Padayachee ER, Zetterberg H, Portelius E, Boren J, Molinuevo JL, Andreasen N, et al. Cerebrospinal fluid-induced retardation of amyloid beta aggregation correlates with Alzheimer's disease and the APOE epsilon4 allele. Brain Res 2016;1651:11–6.

[36] Yu Y, Sheth N, Krishnamoorthy P, Saboury B, Raper A, Baer A, et al. Aortic vascular inflammation in psoriasis is associated with HDL particle size and concentration: a pilot study. Am J Cardiovasc Dis 2012; 2:285–92.

[37] Shuhei N, Soderlund S, Jauhiainen M, Taskinen MR. Effect of HDL composition and particle size on the resistance of HDL to the oxidation. Lipids Health Dis 2010;9:104.

[38] Vekic J, Kotur-Stevuljevic J, Jelic-Ivanovic Z, Spasic S, Spasojevic-Kalimanovska V, Topic A, et al. Association of oxidative stress and PON1 with LDL and HDL particle size in middle-aged subjects. Eur J Clin Invest 2007;37:715–23.

[39] Tesseur I, Van Dorpe J, Spittaels K, Van den Haute C, Moechars D, Van Leuven F. Expression of human apolipoprotein E4 in neurons causes hyperphosphorylation of protein tau in the brains of transgenic mice. Am J Pathol 2000;156:951–64.

[40] Alexander S, Kerr ME, Kim Y, Kamboh MI, Beers SR, Conley YP. Apolipoprotein E4 allele presence and functional outcome after severe traumatic brain injury. J Neurotrauma 2007;24:790–7.

[41] Sen A, Nelson TJ, Alkon DL. ApoE isoforms differentially regulates cleavage and secretion of BDNF. Mol Brain 2017;10:19.